Characteristic Analysis of Coupled HTS Interconnects with Two-Dimensional FDTD

Jun-Fa Mao, *Senior Member, IEEE*, Xiaoning Qian, and Zhengyu Yuan

***Abstract*—In this letter, the frequency-dependent RLGC parameters of high-speed coupled high T_c superconductor (HTS) interconnects are extracted with a two-dimensional (2-D) FDTD algorithm. The response signals of an HTS interconnect circuit and a normal Al interconnect circuit are simulated and compared, showing that not only the signal dispersion, delay, and magnitude decay of HTS interconnects are smaller than that of Al interconnects, the crosstalk of HTS interconnects is much smaller, too.**

***Index Terms*—Crosstalk, HTS interconnect, RLGC parameters, 2-D FDTD.**

I. Introduction

UE TO its better performance than normal conductors, high T_c superconductor (HTS) has attracted much attention recently. The performance of HTS used in microwave and millimeter-wave devices has been analyzed [1]. With low dispersion, high sensitivity, and higher frequency of operation, HTS shows its potential in those applications. Simultaneously, with the increasing speed and integration density of modern integrated circuits, interconnects become more and more crucial to decide the circuit performance. Since the HTS minimum wire size is not limited by resistance considerations, the dimensions of system can be reduced with HTS interconnects. Improved speed is then obtained through scaling down the chip feature size. In order to exploit the characteristics of high-speed HTS interconnects, different approaches have been applied to calculation of the propagation characteristics of HTS interconnects [2]–[4]. However, almost all of the past work was concentrated on single-conductor HTS interconnects. The crosstalk problem of coupled HTS interconnects is still an open issue to study. Further more, the obtained characteristic parameter in the past is the complex propagation constant ($\gamma = \alpha + j\beta$), which is not proper for circuit simulation use. In this letter, the frequency-dependent RLGC parameters of two-conductor coupled HTS interconnects are extracted for the first time with a two-dimensional (2-D) FDTD algorithm. The response of a high-speed HTS interconnect circuit is simulated to highlight the electrical performance advantage of coupled HTS interconnects. The result is compared with a circuit of the same topology but in which the HTS interconnect is substituted with an Al interconnect. It is shown that not only the signal dispersion, delay, and decay of HTS interconnects are much smaller, the crosstalk of HTS interconnects is obviously lower as well.

Manuscript received September 12, 2000; revised November 16, 2000. This work was supported by National Science Foundation for the Outstanding Young of China (60025103) and NSFC (69971015).

The authors are with the Department of Electronic Engineering, Shanghai Jiao Tong University, Shanghai 200030, China (e-mail: jfmao@info.sh.cn).

Publisher Item Identifier S 1531-1309(01)01970-5.

II. Parameter Extraction with 2-D FDTD

For high-speed HTS interconnects, the superconductor thickness is much larger than the penetration depth at working frequency, while in FDTD methods the grids inside the superconductor should be much smaller than the penetration depth. For this reason, the traditional three-dimentional FDTD requires a huge memory storage. Instead, with the compact 2-D FDTD approach [5], [6], only the cross section of an interconnect needs to be meshed with grid cells, saving much computer memory and CPU time. Thus, 2-D FDTD is selected to simulate the electromagnetic (EM) fields for HTS interconnects in this letter. With the two fluid model of HTS, the basic equation for E_x field for a given β as the specified propagation constant is

$$\frac{\partial E_x}{\partial t} = \frac{1}{\varepsilon}\left(\frac{\partial H_z}{\partial y} + \beta H_y - \sigma_n E_x - J_{sx}\right) \tag{1}$$

where σ_n is the normal conductivity, J_{sx} is the x-component of superconductor fluid current density J_s, which relates the electric field by

$$\frac{\partial J_{sx}}{\partial t} = \frac{1}{\mu\lambda_L^2} E_x \tag{2}$$

in which λ_L is the London penetration depth. The difference form of (1) with 2-D FDTD is shown in (3) at the bottom of the next page. In (3), the superconducting fluid current density $J_{sx}^{n+1/2}(i+1/2, j)$ can be calculated from (2) with central-difference approximation for the time derivative

$$J_{sx}^{n+1/2}(i+1/2, j) = J_{sx}^{n-1/2}(i+1/2, j) + \frac{1}{\mu\lambda_L^2(T)} \cdot E_x^n(i+1/2, j). \tag{4}$$

The 2-D difference equations for the other EM fields can be derived in a similar way. After launching an excitation pulse and obtaining the response EM fields for a small number of FDTD time steps, the modal frequency, attenuation constant and EM fields at the remaining time steps for each given propagation constant β can be derived by an optimization method [6].

Only symmetrical two-conductor coupled interconnects are considered for simplicity. In this case, the 2-D FDTD method is used to simulate the EM fields under the even and odd mode excitation separately. Defining V_e and $I_e$as the even mode voltage

and current, $V_o$and I_o as the odd mode voltage and current, respectively, according to the even-odd mode theory we have

$$\begin{bmatrix}\gamma_e(\omega)\cdot V_e(\omega)\\ \gamma_o(\omega)\cdot V_o(\omega)\end{bmatrix} = \begin{bmatrix}Z_{11}(\omega)+Z_{12}(\omega) & 0\\ 0 & Z_{11}(\omega)-Z_{12}(\omega)\end{bmatrix}\begin{bmatrix}I_e(\omega)\\ I_o(\omega)\end{bmatrix} \tag{5a}$$

$$\begin{bmatrix}\gamma_e(\omega)\cdot I_e(\omega)\\ \gamma_o(\omega)\cdot I_o(\omega)\end{bmatrix} = \begin{bmatrix}Y_{11}(\omega)+Y_{12}(\omega) & 0\\ 0 & Y_{11}(\omega)-Y_{12}(\omega)\end{bmatrix}\begin{bmatrix}V_e(\omega)\\ V_o(\omega)\end{bmatrix} \tag{5b}$$

where $\gamma_e(\omega)$ and $\gamma_o(\omega)$ are the complex propagation constants for even mode and odd mode, respectively, Z_{11} and Z_{12} are elements of the impedance matrix $[Z(\omega)] = [R(\omega)] + j\omega[L(\omega)]$, Y_{11}, and Y_{12} are elements of the conductance matrix $[Y(\omega)] = [G(\omega)] + j\omega[C(\omega)]$. Once the dispersion curves of the even and odd mode propagation constants, voltages and currents have been obtained, the frequency-dependent resistance matrix $[R(\omega)]$, inductance matrix $[L(\omega)]$, conductance matrix $[G(\omega)]$, and capacitance matrix $[C(\omega)]$ can be solved from (5).

III. Performance Comparison of HTS and AL Interconnects

A coupled YBCO interconnect shown in the inset of Fig. 1 was analyzed. The conductor width is $w = 2$ μm, conductor thickness is $t = 0.5$ μm, conductor separation is $s = 2$ μm, and the medium height is $h = 1$ μm. The YBCO has penetration depth $\lambda_L(0K) = 0.14$ μm, normal conductivity $\sigma_n(T_c) = 2.08\times 10^6$ S/m and critical temperature $T_c = 92.5$K. The computation temperature is $T = 77$K, at which the frequency independent penetration depth and the normal conductivity are 0.2 μm and 1.0×10^6 S/m, respectively. The obtained $[L(\omega)]$ and $[R(\omega)]$ matrices are given in Figs. 1 and 2. As a comparison, also shown in the figures are the $[L(\omega)]$ and $[R(\omega)]$ matrices of an Al interconnect with the same structure and size as the YBCO interconnect. The conductance and capacitance matrices of both the YBCO and Al interconnects are not shown for briefness.

At last, a circuit shown in Fig. 3 is simulated to highlight the advantage of superconductors as coupled interconnects for high-speed integrated circuits. The two-conductor interconnect

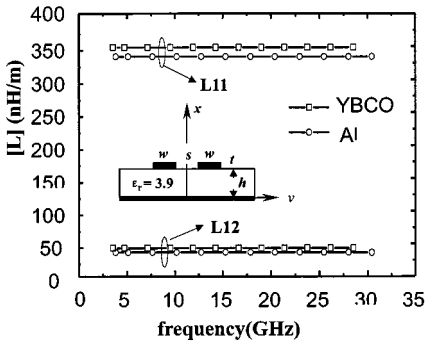

Fig. 1. Cross section view and the inductance matrices of a YBCO interconnect and an Al interconnect.

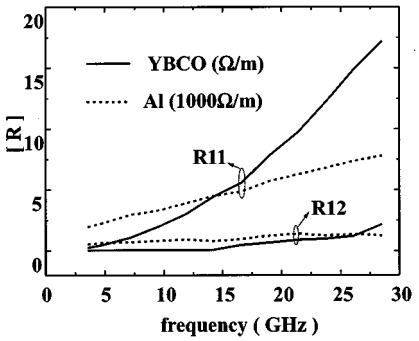

Fig. 2. Resistance matrices of the YBCO interconnect and the Al interconnect shown in Fig. 1

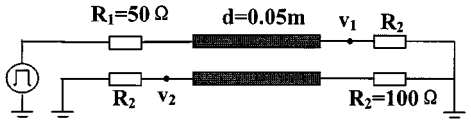

Fig. 3. Example circuit for simulation.

in this circuit has the same cross section structure as that in Fig. 1. The simulation has been performed for two cases, one is that the interconnect conductors are YBCO superconductors and another is that the interconnect conductors are normal Al conductors. The obtained response voltages are given in Fig. 4, from which we can see that the signal dispersion, delay and magnitude decay of the superconductor interconnect are much smaller than that of the Al interconnect. Especially, the crosstalk voltage of the superconductor interconnect is much smaller as

$$E_x^{n+1}(i+1/2,\,j) = \frac{1-\dfrac{\sigma_n\Delta t}{2\varepsilon}}{1+\dfrac{\sigma_n\Delta t}{2\varepsilon}}E_x^n(i+1/2,\,j) + \frac{\dfrac{\Delta t}{\varepsilon}}{1+\dfrac{\sigma_n\Delta t}{2\varepsilon}} \cdot\left[\beta H_y^{n+1/2}(i+1/2,\,j)+\frac{H_z^{n+1/2}(i+1/2,\,j+1/2)-H_z^{n+1/2}(i+1/2,\,j-1/2)}{\Delta y}-J_{sx}^{n+1/2}(i+1/2,\,j)\right] \tag{3}$$

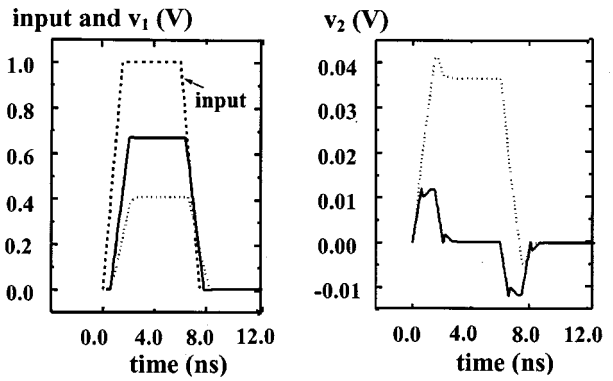

Fig. 4. Input and response voltages in the example cirucit. Solid line: YBCO; Dashed line: Al.

well, which can be explained mainly from the much smaller relative value of mutual resistance $R_{12}(\omega)$ of the superconductor interconnect.

IV. Conclusion

A full-wave analysis method, based on the compact 2-D FDTD, is presented for extraction of the RLGC parameters of coupled HTS interconnects. The obtained frequency-dependent circuit parameters can be inserted into the general simulation software to calculate the time-domain response of interconnect circuits. Better electrical performance, especially lower crosstalk, of coupled HTS interconnects is demonstrated by circuit simulation. The application of HTS conductors as high-speed VLSI interconnects is predicted to be promising.

References

[1] K. S. Kong, H. Y. Lee, and T. Itoh, "Analysis of superconducting microstrip lines," in *IEEE MTT-S Dig.*, 1990, pp. 793–797.

[2] E. B. Ekholm and S. W. McKnight, "Attenuation and dispersion for high-T_c superconducting microstrip lines," *IEEE Trans. Microwave Theory Tech.*, vol. 38, pp. 387–395, Apr. 1990.

[3] M. A. Megahed and S. M. Ghazaly, "Analysis of anisotropic high temperature superconductor planar structures on sapphire anisotropic substrates," *IEEE Trans. Microwave Theory Tech.*, vol. 43, pp. 1989–1992, Aug. 1995.

[4] J. Kang, R. Han, X. Liu, and Y. Wang, "Propagation characteristics of high-T_c superconducting interconnect for VLSI packaging predicted by a generalized two-fluid model," *IEEE Trans. Appl. Superconduct.*, vol. 7, pp. 27–32, Mar. 1997.

[5] S. Xiao and R. Vahldieck, "An efficient 2-D FDTD algorithm using real variables," *IEEE Microwave Guided Wave Lett.*, vol. 3, pp. 127–129, May 1993.

[6] Z.-Y. Yuan and Z.-F. Li, "Efficient computation of frequency-dependent-parameters for on-chip interconnects via two-dimensional FDTD and time signal prediction technique," *IEEE Trans. Adv. Packag.*, vol. 22, pp. 665–673, Nov. 1999.